Journal of Systems Engineering and Electronics
Vol. 29, No. 6, December 2018, pp.1158 – 1169

Adaptive block greedy algorithms for receiving multi-narrowband signal in compressive sensing radar reconnaissance receiver

ZHANG Chaozhu[1, *], XU Hongyi[1], and JIANG Haiqing[2]

1. School of Information and Communication Engineering, Harbin Engineering University, Harbin 150001, China;
2. School of Information and Electronics, Beijing Institute of Technology, Beijing 100081, China

Abstract: This paper extends the application of compressive sensing (CS) to the radar reconnaissance receiver for receiving the multi-narrowband signal. By combining the concept of the block sparsity, the self-adaption methods, the binary tree search, and the residual monitoring mechanism, two adaptive block greedy algorithms are proposed to achieve a high probability adaptive reconstruction. The use of the block sparsity can greatly improve the efficiency of the support selection and reduce the lower boundary of the sub-sampling rate. Furthermore, the addition of binary tree search and monitoring mechanism with two different supports self-adaption methods overcome the instability caused by the fixed block length while optimizing the recovery of the unknown signal. The simulations and analysis of the adaptive reconstruction ability and theoretical computational complexity are given. Also, we verify the feasibility and effectiveness of the two algorithms by the experiments of receiving multi-narrowband signals on an analog-to-information converter (AIC). Finally, an optimum reconstruction characteristic of two algorithms is found to facilitate efficient reception in practical applications.

Keywords: compressive sensing (CS), adaptive greedy algorithm, block sparsity, analog-to-information convertor (AIC), multi-narrowband signal.

DOI: 10.21629/JSEE.2018.06.05

1. Introduction

Since being presented, the compressive sensing (CS) [1 – 3] has gained popularity in recent years. It allows the signal to be obtained far below the Nyquist rate from the non-adaptive linear projections by the optimization algorithm with a sparsity constraint. After a great development, CS has been applied to many research fields, including communication, radar, image processing and biomedicine [4 – 7], studying the feasibility of applications of CS in analog information acquisition.

The essence of the reception process in the analog signal CS is compressed sampling and reconstruction. In terms of compressed sampling, the presentation of the analog-to-information converter (AIC) [8 – 11] successfully connects the digital CS theory to analog implementation. Treichler et al. came up with a design of wideband signal acquisition receiver [12]. In order to blind sub-Nyquist sampling of multiband signals, the modulated wideband conversion (MWC) [13] and quadrature analog-to-information converter (QAIC) [14] were presented successively. They are essentially different parallel structures of the AIC.

For the reconstruction process, many existing algorithms have been presented such as the convex optimization method [15,16] and the greedy algorithm [17]. In the practical application, we are concerned about the greedy algorithm due to its few calculations and flexible settings. Tropp et al. demonstrated theoretically and empirically that the orthogonal matching pursuit (OMP), a fundamental greedy algorithm, can reliably recover a signal [18]. Since the sparse levels required for refactoring are usually unknown or cannot be accurately obtained in many cases, Do et al. presented the sparsity adaptive matching pursuit (SAMP) [19]. It adopts a stepping adaptive method to estimate the sparsity and the true support set without prior information. Malloy et al. proposed an adaptive sensing and group testing algorithm which has good performance in a low signal to noise ratio (SNR) [20]. In [21], the extended orthogonal matching pursuit methods were presented, which use the redundant iterations to increase the probability of successful reconstruction. On the other hand, some studies have proposed reconstruction algorithms specially for the original signal which has special structure. By analyzing characteristic of block sparse signals, Eldar et al. developed the block-MP and the block-OMP (BOMP) algorithm [22,23]. Combining the BOMP with the adaptive

Manuscript received January 08, 2018.
*Corresponding author.
This work was supported by the National Natural Science Foundation of China (61172159).

support method, the block sparsity adaptive matching pursuit (BSAMP) algorithm was proposed [24]. However, this algorithm still needs to know the block length. Hedge et al. extended the CS theory to pulse stream data [25]. Overall, the use of the adaptive methods and the signal structure information can make the algorithm more practical and efficient.

In the context of radar reconnaissance receivers, a large reception bandwidth is required. However, the actual signal is usually distributed only in several narrow bands, which provides the feasibility and necessity for CS receiving. The CS architecture can effectively reduce the sampling pressure of the wideband receiver. However, the existing reconstruction algorithms are mostly applicable to the finite information rate signal, which is not satisfactory in the multi-narrowband signal with continuous spectral characteristics. In addition, the signal which reconnaissance receiver needs to face is completely unknown. Therefore, the reconstruction process needs to have superior adaptability. Based on the above two problems, we propose two adaptive block greedy algorithms called the binary tree search and monitoring block orthogonal matching pursuit (BTS-MBOMP) and the binary tree search block adaptive matching pursuit (BTS-BAMP). Both algorithms can achieve adaptive reconstruction of multi-narrowband signals without the prior sparsity level. And the latter is the improved backtracking version of the former.

Our contributions can be summarized as follows: First, according to the block-occupied feature of the multi-narrowband signal, we organically combine the block sparsity into CS architecture to improve the probability of exact reconstruction and further reduce the lower boundary of the sub-sampling rate. Second, a binary tree search and monitoring mechanism is proposed to solve the adaptive problem of the block size in the block greedy algorithm. This mechanism can accumulate the reconstruction information and effectively remove wrong results when the block size is mismatched. Also, the instability of reconstruction caused by the fixed block length can be overcome. Third, the adaptive reconstruction ability and computational complexity of the proposed algorithms are evaluated and analyzed. Fourth, we validate the feasibility and effectiveness of algorithms by simulating the entire reception and reconstruction process through an AIC structure in different SNRs. Finally, the optimal reconstructed characteristic which can facilitates practical application is found.

The rest of this paper is organized as follows. Section 2 depicts the mathematical CS model based on block sparsity. Search and monitoring mechanism and detailed algorithmic descriptions are provided in Section 3. Finally, performance analysis, scenario simulation and discussion are shown in Section 4, followed by the conclusion in Section 5.

2. Block sparsity and block-CS model

CS focuses on how to recover a signal $\boldsymbol{x}$ of size $N\times 1$ from an observation vector $\boldsymbol{y}$ of size $M \times 1$ with $M \ll N$. The basic CS model is

$$\boldsymbol{y} = \boldsymbol{\Phi x} \tag{1}$$

where $\boldsymbol{\Phi}$ is an $M \times N$ observation matrix which is independent of signal $\boldsymbol{x}$. Since $\boldsymbol{\Phi}$ has much fewer rows than columns, recovering $\boldsymbol{x}$ from $\boldsymbol{y}$ is an undetermined problem that has infinite solutions. Therefore, CS exploits the sparsity of $\boldsymbol{x}$ to make the solution unique and ensure that the mapping between $\boldsymbol{y}$ and $\boldsymbol{x}$ is one-to-one [26]. For sparseness, it is assumed that

$$\boldsymbol{x} = \boldsymbol{\Psi s} \tag{2}$$

where $\boldsymbol{s}$ is a sparse vector of size $N\times 1$ with only k nonzero values. This type of signal $\boldsymbol{x}$ is said to be k-sparse in $\boldsymbol{\Psi}$, and $\boldsymbol{\Psi}$ is called the basis matrix of a transform domain. Combining (1) and (2), $\boldsymbol{y}$ can be rewritten as

$$\boldsymbol{y} = \boldsymbol{\Phi\Psi s} = \boldsymbol{\Theta s} \tag{3}$$

where $\boldsymbol{\Theta} = \boldsymbol{\Phi\Psi}$ is an $M \times N$ recovery matrix. Under sparse constraints, the refactoring process can be described as

$$\widehat{\boldsymbol{s}} = \arg\min \|\boldsymbol{s}\|_0 \ \text{ s.t. } \boldsymbol{\Theta s} = \boldsymbol{y}. \tag{4}$$

In many cases, the sparse expression $\boldsymbol{s}$ of the signal $\boldsymbol{x}$ has block structure. Assuming that $\boldsymbol{s}$ is composed of several blocks with length d_l $(1 \leqslant l)$ respectively

$$\boldsymbol{s} = [\underbrace{s_1, \ldots, s_{d_1}}_{\boldsymbol{s}[1]}, \ldots, \underbrace{s_{N-d_L+1}, \ldots, s_N}_{\boldsymbol{s}[L]}] \tag{5}$$

where $\boldsymbol{s}[l]$ denotes the lth sub-blocks. A block K-sparse signal $\boldsymbol{x}$ is defined as $\|\boldsymbol{s}\|_{2,0} \leqslant K$, where $\|\boldsymbol{s}\|_{2,0}$ is described as

$$\|\boldsymbol{s}\|_{2,0} = \sum_{i=1}^{L} \xi(\|\boldsymbol{s}[i]\|_2 > 0). \tag{6}$$

Note that $\|\boldsymbol{a}\|_2$ stands for the Euclidean norm of the vector $\boldsymbol{a}$, and ξ is an indicator function. $\xi(A) = 1$ if the condition A is satisfied and 0 otherwise.

Similar to the typical k-sparse signal which has at most k nonzero values, the nonzero values of a block sparse signal distribute only in K blocks. Moreover, when $d_1 = \cdots = d_L = d$, the signal is said to be the uniform block sparse, which can be expressed as

$$\boldsymbol{s} = [\underbrace{s_1, \ldots, s_d}_{\boldsymbol{s}[1]}, \underbrace{s_{d+1}, \ldots, s_{2d}}_{\boldsymbol{s}[2]}, \ldots, \underbrace{s_{N-d+1}, \ldots, s_N}_{\boldsymbol{s}[L]}]. \tag{7}$$

Simultaneously, $\boldsymbol{\Psi}$ and $\boldsymbol{\Theta}$ can be successively partitioned into block distribution $\Gamma = \{d_1 = \cdots = d_L = d\}$

similar to $\boldsymbol{s}$ as

$$\boldsymbol{\Psi}=[\underbrace{\varphi_1,\ldots,\varphi_d}_{\boldsymbol{\Psi}[1]},\underbrace{\varphi_{d+1},\ldots,\varphi_{2d}}_{\boldsymbol{\Psi}[2]},\cdots,\underbrace{\varphi_{N-d+1},\ldots,\varphi_N}_{\boldsymbol{\Psi}[L]}] \tag{8}$$

$$\boldsymbol{\Theta}=[\underbrace{\phi_1,\ldots,\phi_d}_{\boldsymbol{\Theta}[1]},\underbrace{\phi_{d+1},\ldots,\phi_{2d}}_{\boldsymbol{\Theta}[2]},\cdots,\underbrace{\phi_{N-d+1},\ldots,\phi_N}_{\boldsymbol{\Theta}[L]}] \tag{9}$$

where $\boldsymbol{\Psi}[i]$ and $\boldsymbol{\Theta}[i]$ $(i=1,2,\ldots,L)$ are the sub-matrices of $\boldsymbol{\Psi}$ and $\boldsymbol{\Theta}$ with size $N\times d$ and $M\times d$, respectively. Substituting (9) and (7) into (3), $\boldsymbol{y}$ can be rewritten as

$$\boldsymbol{y}=(\boldsymbol{\Theta}[1]\boldsymbol{\Theta}[2]\cdots\boldsymbol{\Theta}[L])(\boldsymbol{s}^{\mathrm{T}}[1]\boldsymbol{s}^{\mathrm{T}}[2]\cdots\boldsymbol{s}^{\mathrm{T}}[L])^{\mathrm{T}}=\sum_{i=1}^{L}\boldsymbol{\Theta}[i]\boldsymbol{s}[i] \tag{10}$$

and the mathematical model (4) can be rewritten as

$$\widehat{\boldsymbol{s}}=\arg\min\|\boldsymbol{s}\|_{2,0},\quad \text{s.t.}\sum_{i=1}^{L}\boldsymbol{\Theta}[i]\boldsymbol{s}[i]=\boldsymbol{y}. \tag{11}$$

The above problems can be solved by the OMP type greedy algorithm. Davenport et al. pointed out the conditions for the exact reconstruction of such algorithms [27]:

Definition 1 Let $\boldsymbol{\Theta}$ be a given matrix. If there exists a restricted isometric constant (RIC) δ_k which satisfies

$$(1-\delta_k)\|\boldsymbol{s}\|_{\ell_2}^2\leqslant\|\boldsymbol{\Theta s}\|_{\ell_2}^2\leqslant(1+\delta_k)\|\boldsymbol{s}\|_{\ell_2}^2 \tag{12}$$

then $\boldsymbol{\Theta}$ satisfies the restricted isometry property (RIP), and $\boldsymbol{s}$ has a unique solution if $\delta_k\in(0,1)$. Eldar et al. generalized the RIP to the block sparsity and proposed block RIP (Block-RIP) [28]:

Definition 2 $\boldsymbol{\Theta}$ satisfies the Block-RIP over $\Gamma=\{d_1,\ldots,d_L\}$ with parameter $\delta_{K|\Gamma}$ if for every $x\in\mathbf{R}^N$ that is block K-sparse, we have

$$(1-\delta_{K|\Gamma})\|\boldsymbol{s}\|_2^2\leqslant\|\boldsymbol{\Theta s}\|_2^2\leqslant(1+\delta_{K|\Gamma})\|\boldsymbol{s}\|_2^2 \tag{13}$$

where $\delta_{K|\Gamma}$ is the RIC of block K-sparse $\boldsymbol{x}$ over Γ. Our previous work [29] proved that block sparsity can reduce the RIC ($\delta_{K|\Gamma}\leqslant\delta_k$), thereby increasing the reconstruction probability and reducing the lower boundary of the sub-sampling rate. The others obvious advantages of the block greedy algorithm are their smaller computational complexity.

3. Adaptive block greedy algorithms

The BOMP [23], combined with block sparsity and OMP type algorithms, achieves a good performance of reconstruction. For practical purpose, Fu et al. proposed the BSAMP which can self-adapt to the block sparsity level K drawing on the ideas of SAMP [24]. Although it does not need to set the block sparsity level in advance, a fixed block length is needed to be given in the initialization. According to our previous studies, different block lengths can bring different effects on the reconstruction. Accuracy loss is unavoidable when the block is unbefitting (mismatch). In addition, the length of each non-zero block will be different when the signal is close to the actual scenario (non-uniform blocks). Therefore, we need an algorithm that can adapt to both block sparsity level and block length.

3.1 Binary tree search and monitoring mechanism

We propose a binary tree search and monitoring mechanism in the process of block support reconstruction. The diagram is shown in Fig. 1. This mechanism can gradually exclude unoccupied sub-blocks and narrow the search domain. The reconstruction can be eventually completed when the block length reduces to a given block resolution. The block supports which have been found in the last search can be used as a priori information to the next search. Also, the search process does not require priori information of signal block size and sparsity level.

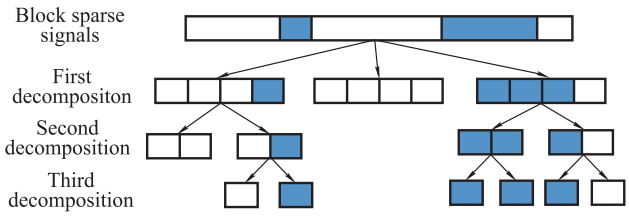

Fig. 1 Decomposition of non-uniform block sparse signal

The idea of binary tree search can be summarized as follows:

(i) First, searching block support in $d=2^h\left(h\leqslant\log_2\dfrac{N}{2}\right)$;

(ii) Segmenting blocks. Searching block support in $d=2^{h-1}$ within the range of block supports which were found previously;

(iii) Repeating (ii) until the block length reduces to the block resolution.

The binary tree search can effectively solve the self-adaptation problem of both block size and block sparsity level. However, the accumulation of prior knowledge may also create risks. A wrong block support will be extended to the after searches, thereby, affect the reconstruction results. Therefore, it is necessary to add a suitable monitoring condition to ensure that each search can obtain the correct block supports. In this paper, we set the monitoring condition as follows. If

$$\|\boldsymbol{r}_s\|_2/\|\boldsymbol{r}_0\|_2\leqslant\lambda, \tag{14}$$

the block supports will be submitted to the next stage as a priori knowledge. $\|\boldsymbol{r}_s\|_2$ and $\|\boldsymbol{r}_0\|_2$ are the standard Euclidean norm of the residuals in h stage ($d = 2^h$) and the original measurements, respectively. Note that $\|\boldsymbol{r}_0\|_2 = \|\boldsymbol{y}\|_2$, and $\lambda \in (0, 1)$ is the monitoring threshold.

If the condition is not satisfied, it means that reconstruction error occurs or the block length is inappropriate. The results will be discarded and the search of the next stage will be directly carried out. The monitoring condition can screen out reliable prior knowledge effectively and exclude the case of mismatch.

3.2 Reconstruction algorithms adaptive to block length and sparsity level

Based on the binary tree search and monitoring mechanism, this paper presents two algorithms adaptive to both block sparsity level and block size. The main difference between the two algorithms is the iterative approach in the search process. They are mainly proposed for receiving unknown multi-narrowband signals in the CS wideband radar reconnaissance receiver. Also, they can be used in many other cases, e.g., spectrum sensing, cognitive radio.

3.2.1 BTS-MBOMP

After solving the adaptive problem, an appropriate block iteration method needs to be selected in each search. BOMP is a good choice due to its simple procedure and good performance. Combining the binary tree search and monitoring with BOMP, we first present an algorithm called the BTS-MBOMP. The diagram is shown in Fig. 2.

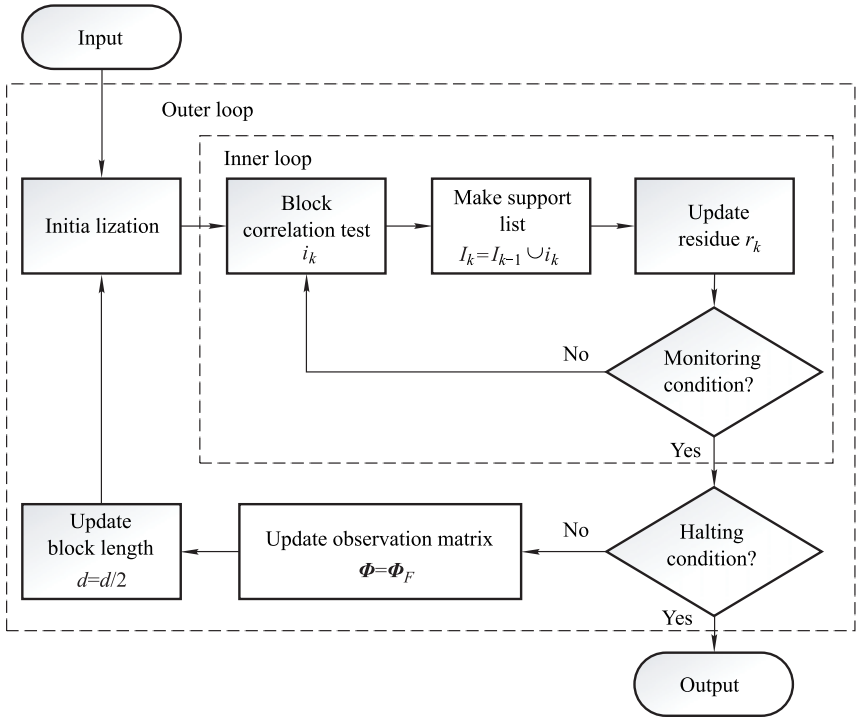

Fig. 2 Diagram of BTS-MBOMP

The pseudo code of the BTS-MBOMP is as follows.

Input: Recovery matrix $\boldsymbol{\Theta}$, sampled vector $\boldsymbol{y}$; decomposition level h;

Output: A block sparse approximation $\widehat{\boldsymbol{x}}$;

Initialization:

$\widehat{\boldsymbol{x}}_0$; {Trivial initialization}

Outer loop

$I_0 = \varnothing$; {Empty finalist}

$k = 1$; {Iteration index}

$\boldsymbol{r}_0 = \boldsymbol{y}$; {Initial residue}

$d = 2^h$; {Stage block length}

$\boldsymbol{\Theta} = [\underbrace{\phi_1, \ldots, \phi_d}_{\boldsymbol{\Theta}[1]}, \ldots, \underbrace{\phi_{N-d+1}, \ldots, \phi_N}_{\boldsymbol{\Theta}[L]}]$; {Block division}

Inner loop

$i_k = \arg\max(\|\boldsymbol{\Theta}^{\mathrm{T}}[i]\boldsymbol{r}_{k-1}\|_2)$; {Block correlation}

$I_k = I_{k-1} \cup i_k$; {Make support list}

$\boldsymbol{r}_k = \boldsymbol{y} - \sum_{i \in I} \boldsymbol{\Theta}_{l_k}[i](\boldsymbol{\Theta}^{\dagger}_{I_k}[i]\boldsymbol{y})$; {Compute residue}

$k = k + 1$; {Update the stage index}

if $\|\boldsymbol{r}_k\|_2 > \|\boldsymbol{r}_0\|_2 \leqslant \gamma$ {Monitoring condition}

then $use = 1$ {Priori identification}
quit the inner loop;
else if $\|\boldsymbol{r}_k\|_2 > 2\|\boldsymbol{r}_0\|_2$ or $|I_k| > M$ {failed}
then $use = 0$ quit the inner loop;
end
Inner loop end
if $\|\boldsymbol{r}_k\|_2 \leqslant \varepsilon$ or $h = 1$ {Halting condition}
then quit the outer loop;
else if $use = 1$
$\boldsymbol{\Theta} = \boldsymbol{\Theta}_{I_k}$; {Update recovery matrix}
end
$h = h - 1$; {Update decomposition level}
Outer loop end
until halting condition true;
Output:
$\widehat{\boldsymbol{x}} = \boldsymbol{\Theta}_{I_k}^{\dagger}\boldsymbol{y}$ {Prediction of non-zero coefficients}

In the outer loop, $\boldsymbol{\Theta}$ is divided by $d = 2^h$ in each search stage, where h is the decomposition level. The inner loop is a BOMP iteration with monitoring condition. Note that $i_k = \arg\max(\|\boldsymbol{\Theta}^{\mathrm{T}}[i]\boldsymbol{r}_{k-1}\|_2)$ means that the block index of maximum $\|\boldsymbol{\Theta}^{\mathrm{T}}[i]\boldsymbol{r}_{k-1}\|_2$ will be selected to the support list. For $\Lambda \in \{1, \ldots, N\}$, $\boldsymbol{\Theta}_{\Lambda}$ is a submatrix of $\boldsymbol{\Theta}$ which only contains block index set Λ. And $\boldsymbol{\Theta}_I^{\dagger} = (\boldsymbol{\Theta}_I^{\mathrm{T}}\boldsymbol{\Theta}_I)^{-1}\boldsymbol{\Theta}_I^{\mathrm{T}}$ is the pseudoinverse of $\boldsymbol{\Theta}_I$.

The inner loop stops iteration by the monitoring condition. When $\|\boldsymbol{r}_s\|_2/\|\boldsymbol{r}_0\|_2 \leqslant \lambda$ is satisfied, a priori information mark $use = 1$ is returned to the outer loop. It means that the block supports having been found are adequate and can already be used as prior knowledge in the next search. Conversely, if $\|\boldsymbol{r}_k\|_2 > \|\boldsymbol{r}_0\|_2$ or the number of supports is greater than measurements, the reconstruction fails and the iteration will be halted to avoid unnecessary calculations. The algorithm skips into the next stage directly.

Decomposition level h: $1 \leqslant h \leqslant \left\lfloor \log_2 / \frac{N}{2} \right\rfloor$, where $\lfloor\ \rfloor$ means rounded down. The decomposition level determines the largest block size in the whole search process. The block length should be greater than or equal to 2 (so $h \geqslant 1$). In order to ensure the reconstruction accuracy and fully reflect the superiority of block sparsity, h should be a relatively large value. A larger h can provide more information at different resolutions. Empirically, the middle part of the range $1 \leqslant h \leqslant \left\lfloor \log_2 / \frac{N}{2} \right\rfloor$ (such as $h = \left\lfloor (\log_2 \frac{N}{2})/2 \right\rfloor$ or $h = \left\lceil (\log_2 \frac{N}{2})/2 \right\rceil$) usually has a better performance.

Halting conditions: Similar to the SAMP, the BTS-MBOMP stops when the norm of residual $\|\boldsymbol{r}\|_2$ is smaller than a certain threshold ε, which means noise energy value for noisy measurements, and $\varepsilon = 0$ in the case of noiseless measurements.

Monitoring conditions: The monitoring threshold $1 > \gamma \geqslant \varepsilon$ is a flexible value. $\|\boldsymbol{r}_k\|_2/\|\boldsymbol{r}_0\|_2$ is a ratio of iteration residual and initial residual, representing the stage degree of completion. A small γ is recommended to ensure the prior information can be accumulated correctly. Based on our experiments, one to three orders of magnitude larger than ε ($\gamma = 10 - 10^3\varepsilon$) is a reliable choice.

3.2.2 BTS-BAMP

The BTS-MBOMP is simple and speedy, but it has an inherent drawback: the selected block can only be added into the final supports unidirectionally but cannot be withdrawn. This causes easier accumulation of error supports and reduces the probability of exact reconstruction. To solve this problem, we propose an improved algorithm, BTS-BAMP. The the diagram is shown in Fig. 3.

The pseudo code of the BTS-BAMP is as follows.

Input: Recovery matrix $\boldsymbol{\Theta}$, sampled vector $\boldsymbol{y}$, decomposition level h; step size w;
Output: A block sparse approximation $\widehat{\boldsymbol{x}}$;
Initialization:
$\widehat{\boldsymbol{x}} = 0$; {Trivial initialization}
Outer loop
$F_0 = \varnothing$; {Empty finalist}
$I = w$; {Size of the finalist in the first stage}
$k = 1$; {Iteration index}
$\boldsymbol{r}_0 = \boldsymbol{y}$; {Initial residue}
$j = 1$; {Stage index}
$d = 2^h$; {Stage block length}
$\boldsymbol{\Theta} = [\underbrace{\phi_1, \ldots, \phi_d}_{\boldsymbol{\Theta}[1]}, \ldots, \underbrace{\phi_{N-d+1}, \ldots, \phi_N}_{\boldsymbol{\Theta}[L]}]$; {Block division}
Inner Loop
$S_k = \arg\max(\|\boldsymbol{\Theta}^{\mathrm{T}}[i]\boldsymbol{r}_{k-1}\|_2, I)$ {Preliminary test}
$C_k = F_{k-1} \cup S_k$ {Make candidate list}
$F = \arg\max(\|\boldsymbol{\Theta}_{C_k}^{\dagger}\boldsymbol{y}\|_2), I)$ {Final test}
$\boldsymbol{r} = \boldsymbol{y} - \boldsymbol{\Theta}_F\boldsymbol{\Theta}_F^{\dagger}\boldsymbol{y}$ {Compute residue}
if $\|\boldsymbol{r}\|_2/\|\boldsymbol{r}_0\| \geqslant \|\boldsymbol{r}_0\|_2 \leqslant \gamma$ {Monitoring condition}
then $use = 1$;
quit the inner loop;
else if $\|\boldsymbol{r}\|_2 \geqslant \|\boldsymbol{r}_{k-1}\|_2$ then {stage switching}
$j = j + 1$ {Update the stage index}
$I = j \times w$ {Update the size of finalist}
else
$F_k = F$ {Update the finalist}
$\boldsymbol{r}_k = \boldsymbol{r}$ {Update the residue}

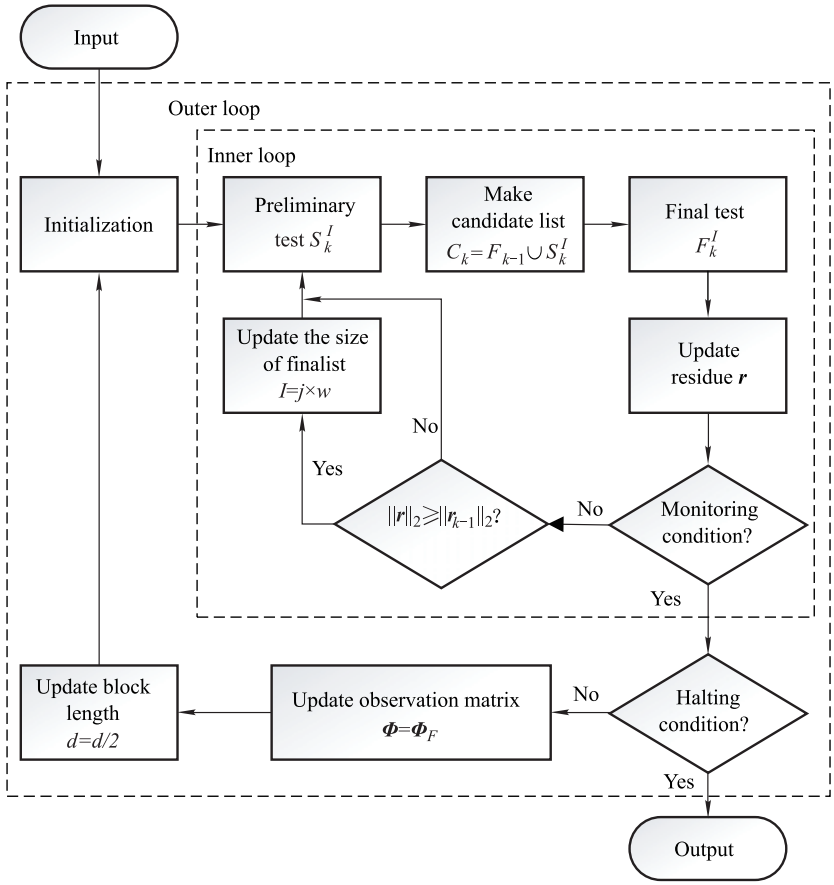

Fig. 3 The diagram of the BTS-BAMP

$k = k + 1$ {Update the stage index}

Inner loop end

if $\|\boldsymbol{r}\|_2 \leqslant \varepsilon$ or $h = 1$ {Halting condition}

then quit the outer loop;

else

$\boldsymbol{\Theta} = \boldsymbol{\Theta}_F$; {Update observation matrix}

$h = h - 1$; {Update decomposition level}

Outer loop end

until halting condition true;

Output:

$\widehat{\boldsymbol{x}} = \boldsymbol{\Theta}_F^{\dagger}\boldsymbol{y}$ {Prediction of non-zero coefficients}

The outer loop is still a binary tree search process with block length $d = 2^h$ in the corresponding search stage. In the inner loop, the support adaptive approach and block backtracking mechanism are added:

(i) The support self-adaptive approach. The main characteristic of this approach is that the size of the support is inconclusive and varied.

The support size in reconstruction is expanded gradually by the product of stage j and step size w which have been set in the initialization.

(ii) The block backtracking mechanism. The primary function of block backtracking is the supports correction. The algorithm firstly selects I block supports in preliminary test and merges this I block supports with other I block supports produced in the previous loop. Then, it uses the method of least squares to choose the best I block supports from candidate sets (containing $2I$ blocks supports) as final supports. In this way, block supports can be selected and removed at the same time. Note that $S_k = \arg\max(\|\boldsymbol{\Theta}^{\mathrm{T}}[i]\boldsymbol{r}_{k-1}\|_2, I)$ means the preliminary test set is constructed by I largest indexes of $\|\boldsymbol{\Theta}^{\mathrm{T}}[i]\boldsymbol{r}_{k-1}\|_2$. Dai et al. pointed out that backtracking mechanism can eliminate the error supports matched in previous iteration, and quickly pick the correct support into the final list [30].

The step size ω is the initial length of S_k and F, and it will control the size of the block support set with the stage index j. The setting of ω is an open-ended question. ω needs to satisfy $1 \leqslant \omega \leqslant K$. If ω increases, the change interval of supports between the two adjacent searches will increase, making the reconstruction more quick but more prone to inaccurate estimation. Therefore, the setting of ω needs to compromise with speed and accuracy. For our intent, multi-narrowband signal, $\omega = 2$ is a more general set since the spectrum is symmetrical.

The setting of the decomposition level, the monitoring condition and the halting condition are similar to the BTS-MBOMP, so the description will not be repeated here.

4. Performance analysis and simulation

This section will analyse and verify the performance of the two adaptive algorithms. Firstly, the adaptive reconstruction capability of the BTS-MBOMP and BTS-BAMP is shown by four simulations of ideal block sparse signals. Then, the computational complexity is analysed and compared. Finally, the typical multi-narrowband signals with noise are chosen to test the practical feasibility and effectiveness of the BTS-MBOMP and BTS-BAMP used in an AIC architecture.

4.1 Adaptive reconstruction capability

In this section, the ideal block sparse signal is used for adaptive capacity assessment. The non-zero blocks are randomly distributed in the signal. The block length is divided into two cases: (i) Uniform block: all blocks have a uniform length $d = 4$; (ii) Non-uniform block: each block is assigned $d = 2, 4, 6$ randomly, but the number of $d = 2$ is the same as $d = 6$ to ensure the total sparsity level is constant. And the amplitude of each block follows the Gaussian and zero-one model respectively. The signal length $N = 512$ and the observation number $M = 128$. The block sparsity level is set from 1 to 90. In order to compare adaptive ability, the SAMP, BOMP and BSAMP are used to reconstruct the same signal simultaneously. Each algorithm performs 500 reconstructions for each K and each signal. According to the instructions of parameter setting in Sections 3.2.1 and 3.2.2, the initialization settings are as Table 1.

Table 1 Initialization settings 1

Algorithm	Block length d	Block sparsity level K	Step size ω	Monitoring condition γ	Decomposition level h	Halting condition ε
SAMP	—	—	4	—	—	10^{-5}
BOMP	4	Given	—	—	—	—
BSAMP	4	—	2	—	—	10^{-5}
BTS-MBOMP	—	—	—	10^{-3}	5	10^{-5}
BTS-BAMP	—	—	2	10^{-3}	5	10^{-5}

The signal itself is block sparse, so the orthogonal basis is a unit matrix. The Gaussian matrix is chosen as the measurement matrix. In this paper, the reconstructed signal $\widehat{\boldsymbol{x}}$ is considered to be exactly restored if $\|\widehat{\boldsymbol{x}} - \boldsymbol{x}\|_2 < 10^{-5}$. The particular interest is the block sparsity level at which the recovery rate starts to drop below 100%, namely the critical block sparsity, which, when exceeded, leads to errors in the reconstruction. The reconstruction results of both cases are shown in Fig. 4. The x-axis in Fig. 4 denotes the sparsity level, while the y-axis represents the percentage of exact recovery. First, we can see that all of the block greedy algorithms have better performance than SAMP, proving the advantages of the block sparsity. On the other hand, the simulation results reveal an interesting phenomenon: the performances of BTS-MBOMP and BTS-BAMP are similar to BOMP and BSAMP respectively in the case of ideal uniform block. However, in the case of non-uniform block, both algorithms are superior to BOMP and BSAMP which need to set a fixed block length or block sparsity level K.

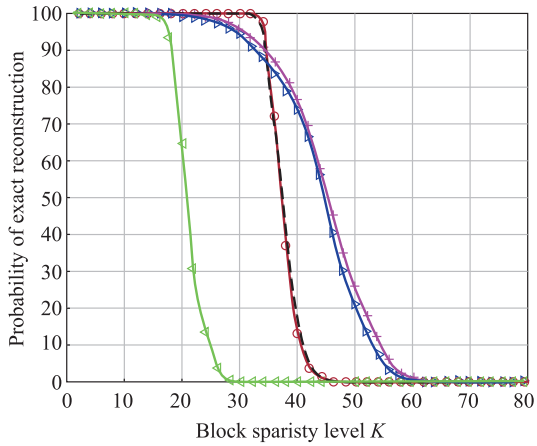

(a) Uniform block with Gaussian model

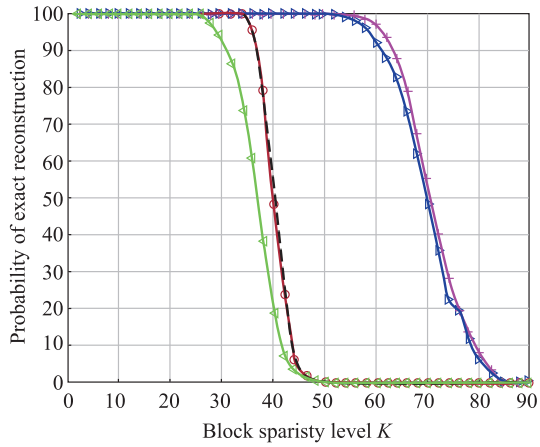

(b) Uniform block with zero-one model

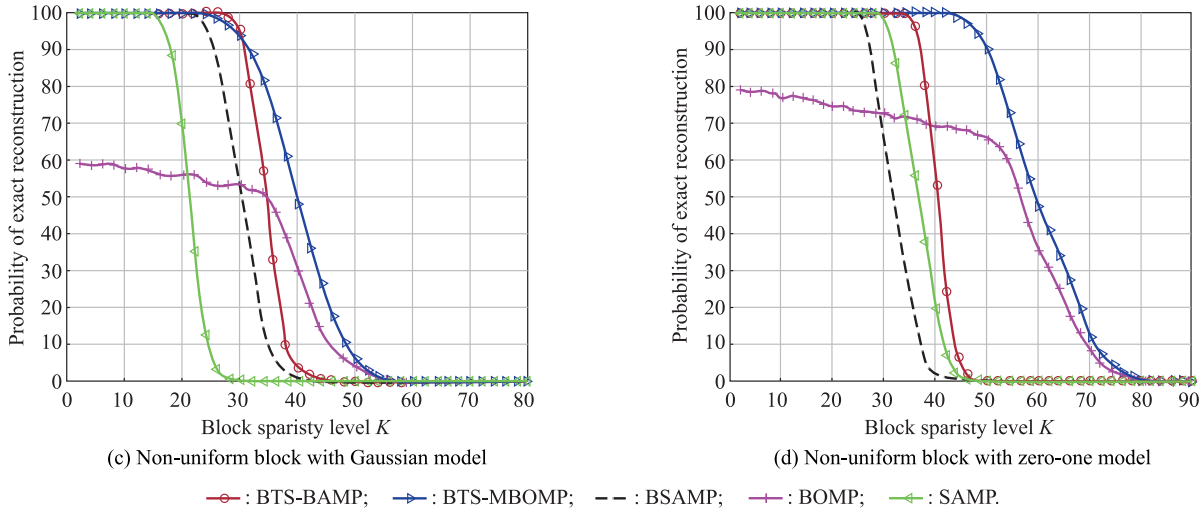

Fig. 4 Simulation results of the exact recovery

In Fig. 4(a) and Fig. 4(b), we set the correct prior information for BOMP and BSAMP, which means that the two algorithms achieve their optimal reconstruction performance in the simulations. If the prior information is set incorrectly at initialization or the actual block is complex, as shown in Fig. 4(c) and Fig. 4(d), the advantages of our proposed algorithm are performed. Therefore, based on the above discussion, the simulation results can exactly prove the adaptive reconstruction capability of the BTS-MBOMP and the BTS-BAMP.

4.2 Computational complexity

Refering to [30], we use the experimental method to analyse the computational complexity of the proposed two algorithms. Fig. 5 shows the relationship between the block sparsity level and the average number of iterations of the two algorithms. To generate the plots of Fig. 5, we set the number of the sub-sampling (observation) $M = 128$ while the signal length $N = 512$. The signal and initialization of the two algorithms are the same as Section 4.1. For each type of the block sparse signal, we select the block sparsity level K from 1 to 30. And for each K, we select 300 different randomly generated Gaussian observation matrices and as many as different support sets.

The number of iterations of the BTS-MBOMP can be easily seen to satisfy $O(K)$ in both types of signals. Also, for BTS-BAMP, the number of iterations conforms $O(\log_2 K)$ when $\omega = K$ but $O(K)$ when $\omega = 1$, although there are some fluctuations in the process of switchover of binary tree search.

After obtaining the number of iterations required for exact reconstruction, the computational complexity of the BTS-MBOMP and the BTS-BAMP can be generally estimated: it equals the complexity of one iteration multiplied by the number of iterations. The complexity of the OMP-type algorithms mainly focuses on the correlation maximization (CM) operation, which requires MN computations in general [30]. And the cost of computing the projections by using the modified Gram-Schmidt (MGS) algorithm is of the order $O(K^2M)$ [31]. For the BTS-MBOMP, because the complexity of the projection is marginal compared with the CM, the algorithm complexity is therefore always $O(MNK)$. For the BTS-BAMP, by combining two extreme situations ($\omega = 1$ and $\omega = K$), the corresponding total complexity can be limited between $O(M(N+K^2)\log_2 K)$ and $O(M(N+K^2)K)$, where the parameter K is the block sparsity level. When the signal is block sparse, K is usually much smaller than practical sparsity level k. Therefore, the computational complexity is also optimistic and acceptable.

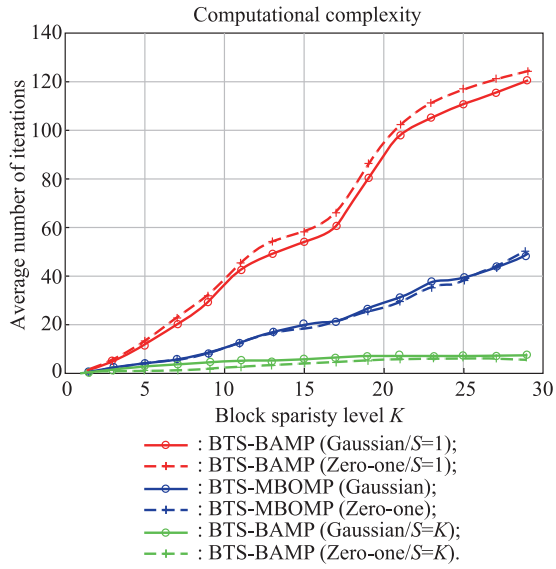

Fig. 5 Iterations of BTS-MBOMP and BTS-BAMP

4.3 Receiving multi-narrowband signal on AIC structure

In the context of engineering practice, we simulate the entire reception and reconstruction process to test the feasibility and effectiveness of our algorithms. The AIC [10], as a successful practice of the analog signal CS, is used to obtain compressive samples from the original signal in our test.

4.3.1 AIC

The physical implementation of a classic AIC is shown in Fig. 6, which includes a mixer for pre-demodulation, a low-pass filter for integral and a low-speed analog-to-digital converter (ADC).

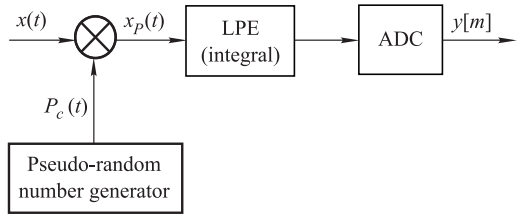

Fig. 6 AIC physical implementation structure

First, the analog signal $x(t)$ is demodulated with $P_c(t)$, where $P_c(t)$ is a pseudo-random sequence of ± 1 with frequency greater than the signal's Nyquist rate. The mathematical expression of $P_c(t)$ is given by

$$P_c(t)=\varepsilon_n,\quad t\in\left[\frac{n}{W},\frac{n+1}{W}\right];$$
$$n=0,1,\ldots,W-1 \tag{15}$$

where ε_n takes ± 1 with equal probability at rate W. Second, the demodulated waveform $x_p(t)$ passes through the low-pass filter $h(t)$ to compress information (integration). Finally, compressive samples $y[m]$ are obtained by a low-rate ADC with sampling period T. The sampling rate of this ADC is much lower than the Nyquist rate. Assuming that the signal $x(t)$ can be expressed as

$$x(t)=\sum_{n=1}^{N}s_n\psi_n(t) \tag{16}$$

where $\boldsymbol{\Psi}=[\psi_1(t),\psi_2(t),\ldots,\psi_N(t)]$ is a set of orthogonal bases. The expression of $y[m]$ can be described as

$$y[m]=\sum_{n=1}^{N}s_n\int_{-\infty}^{\infty}\psi_n(\tau)p_c(\tau)h(mT-\tau)\mathrm{d}\tau. \tag{17}$$

Comparing (17) with CS model (3), the recovery matrix $\boldsymbol{\Theta}$ can be written as

$$\theta_{m,n}=\int_{-\infty}^{\infty}\psi_n(\tau)p_c(\tau)h(mT-\tau)\mathrm{d}\tau. \tag{18}$$

The random demodulation based AIC is a simple but ingenious structure which can fully reflect the CS architecture in the analog domain. In this paper, we use a single branch AIC for signal sub-sampling.

4.3.2 Feasibility and effectiveness

We choose the typical ideal multi-narrowband signal with noise as the original signal. In order to simulate the unknown situation of received signals, the original input is generated with random carrier frequency, bandwidth and energy coefficient in a controllable range. The signal model is given by

$$x(t)=\sum_{i=1}^{L}E_i\cdot\mathrm{sinc}(B_i(t-\tau_i))\cdot$$
$$\cos(2\pi f_i(t-\tau_i))+n(t) \tag{19}$$

where the number of sub-bands is set to $L=4$, the time offsets are set to $\tau_i=[0.7,0.3]$, the energy coefficients E_i are generated randomly in $(0,10]$, and the sub-band bandwidth B_i are selected randomly in $(0,2]$ MHz. The simulation sampling rate is $f_s=100$ MHz. Also, the Nyquist rate is $f_{\mathrm{Nyq}}=f_s/2$ MHz, and the carrier frequency f_i is generated randomly in $[\max B_i,(f_{Nyq}/2)-\max B_i]$ MHz. We set the signal length to $N=2\ 048$. Note that $n(t)$ is white Gaussian noise. The SNR is divided into: (i) Ideal signals without noise; (ii) SNR $=30$ dB; (iii) SNR $=20$ dB; (iv) SNR $=10$ dB.

Since our purpose is to receive the multi-narrowband signal, the frequency domain can be considered to be the sparse transform domain in CS naturally. Although the spectrum of $x(t)$ is not strictly sparse, especially with noise, it can be defined as a compressible signal [32]. Based on the above considerations, we use discrete Fourier transform (DFT) basis as the sparse basis $\boldsymbol{\Psi}$ in the CS. The number of sub-sampling M is set from 50 to 900 with the interval of 10.

In the reconstructed part, we recover the signals from $y[m]$ respectively by five algorithms: the SAMP, the BOMP, the BSAMP, the BTS-MBOMP and the BTS-BAMP. In addition to the BOMP, the rest of the algorithms are all adaptive algorithms (BOMP is proved ineffective with unknown and irregular blocks in Section 4.1, therefore, we only use it in the ideal signal for comparison). Each algorithm performs 500 Monte Carlo simulations for each M and SNR.

The initialization settings are shown in Table 2, where '—' means that this parameter is not required, and the block sparsity level of the BOMP need be measured after signals are generated. The simulation results can be seen in Fig. 7.

Table 2 Initialization settings 2

Algorithm	Block length d	Block sparsity level K	Step size ω	Monitoring condition γ	Decomposition level h	Halting condition ε
SAMP	—	—	10	—	—	10^{-5}
BOMP	10	Measuring	—	—	—	—
BSAMP	10	—	2	—	—	10^{-5}
BTS-MBOMP	—	—	—	10^{-3}	8	10^{-5}
BTS-BAMP	—	—	2	10^{-3}	8	10^{-5}

Under the ideal scene, as shown in Fig. 7(a), the reconstruction probability of two proposed algorithms is gradually better than others with the increase of M. Consistent with the theoretical expectations, the BTS-BAMP has more excellent accuracy than the BTS-MBOMP due to the support self-adaptive approach and block backtracking mechanism. For the BOMP, its probability curve has obvious fluctuation. This phenomenon is caused by the fact that the observation matrix cannot be segmented by the fixed block length appropriately. For example, $d = 10$ while $M = 305$. The part which cannot be completely divided needs to reconstruct a completed block with several measurements in previous block.

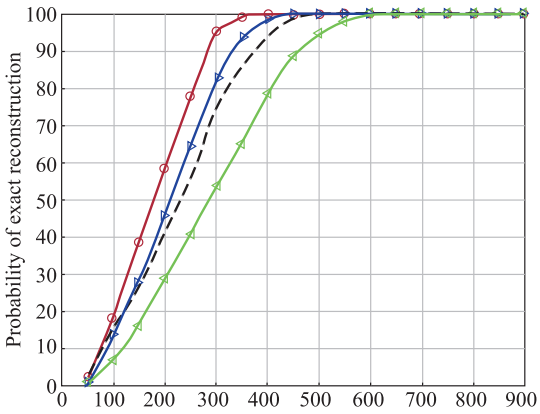

(a) Ideal reconstruction without noise

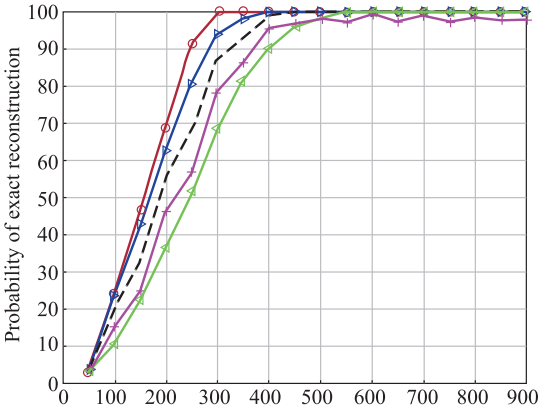

(b) Reconstruction in SNR=30 dB

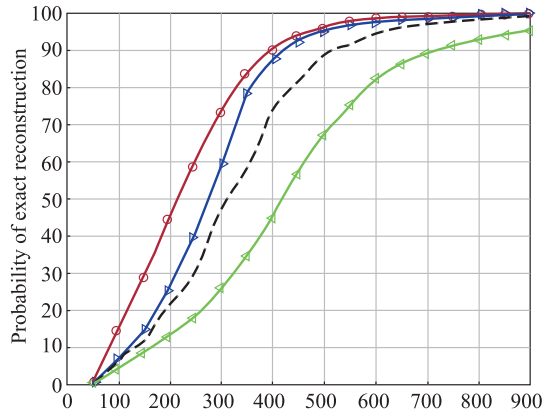

(c) Reconstruction in SNR=20 dB

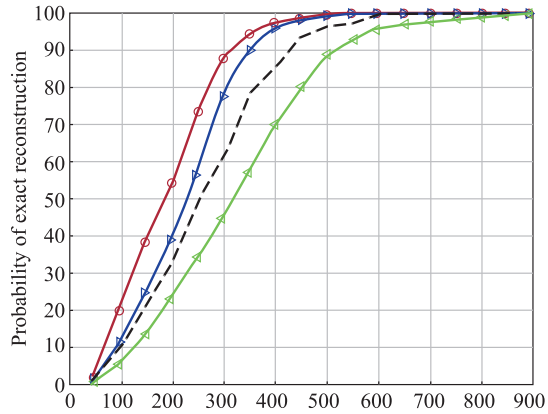

(d) Reconstruction in SNR=10 dB

: BTS-BAMP; : BTS-MBOMP; : BSAMP; : SAMP.

Fig. 7 Simulation results of reconstruction probability

The same operation on the observation matrix increases the block correlation, thus reducing the probability of exact reconstruction. The BSAMP, which is also limited by the fixed block length, is also affected by this unstable factor. In this sense, we can see the binary tree search and monitoring mechanism can effectively improve stability and adaptability.

When in the noise environment, the advantages of the proposed algorithm become more obvious. Fig. 7(b)–Fig. 7(d) show the good ability of the BTS-MBOMP and the BTS-BAMP to handle complex block sparse situations.

Also, benefit from the supports self-adaptive approach and the backtracking mechanism, the BTS-BAMP is more tolerant to the noise than BTS-MBOMP at low sub-sampling rates.

4.3.3 Optimum reconstruction characteristic

We record the simulation time to approximate the trends of practical calculation between different algorithms. The Intel Core i3-3220 CPU and 8G RAM are used to run the Matlab R2015b.

As shown in Fig. 8, it is interesting to note that the reconstructed time of the BTS-MBOMP and the BTS-BAMP have a common tendency. These curves first rise rapidly, then drop to the local minimum, and rise linearly again. Also, the local minimum point of the two algorithms corresponds to 100% reconstruction probability exactly. This is caused by the monitoring condition of information accumulation process. According to this feature, we consider M which corresponds to the local minimum reconstruction time as the optimal sub-sampling number. The corresponding sampling rate is called the optimal reconstruction sub-sampling rate. When the AIC operates at this sub-sampling rate, the proposed algorithms have reliable performance with highest reconstruction efficiency. The optimal reconstruction states of these two algorithms are only related to the bandwidth range, energy range, and the possible frequency range of narrowband signals. If it is possible to estimate the above three parameters before receiving the signal or we simply receive signals within a certain range, the appropriate sub-sampling rate of the CS radar reconnaissance receiver can be set by the optimum reconstruction characteristic.

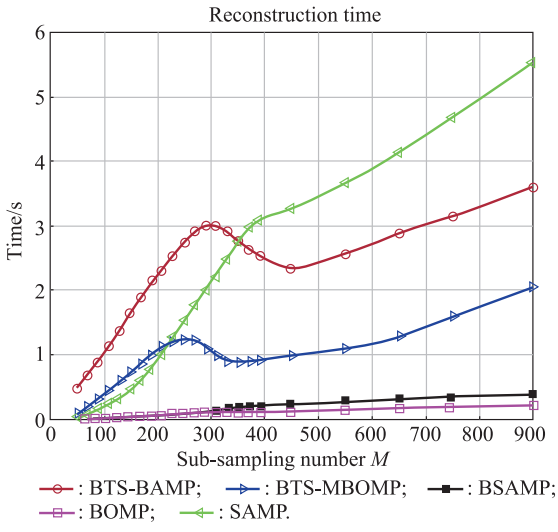

Fig. 8 Simulation results of reconstruction time

5. Conclusions

Combining the concept of the block sparsity, the block supports self-adaption methods, the binary tree search, and the monitoring mechanism, we propose two adaptive algorithms, named the BTS-MBOMP and the BTS-BAMP for receiving multi-narrowband signals on the CS architecture radar reconnaissance receiver. The two proposed algorithms can perform high probability adaptive reconstruction of unknown signals. Their practical refactoring performance can approximate or be better than the optimal case of the BOMP and the BSAMP. Although the proposed algorithms use more calculations in exchange for accuracy, the computational complexity still has the advantage when the signal has block sparse structures. Finally, the feasibility and effectiveness of the algorithms applied to the AIC are confirmed, while an optimum reconstruction characteristic is found to facilitate efficient reception in practical applications.

References

[1] DONOHO D L. Compressed sensing. IEEE Trans. on Information Theory, 2006, 52(4): 1289 – 1306.
[2] CANDES E J, ROMBERG J, TAO T. Robust uncertainty principles: exact signal reconstruction from highly incomplete frequency information. IEEE Trans. on Information Theory, 2006, 52(2): 489 – 509.
[3] CANDES E J, WAKIN M B. An introduction to compressive sampling. IEEE Signal Processing Magazine, 2008, 25(2): 21 – 30.
[4] TROPP J A, LASKA J N, DUARTE M F, et al. Beyond Nyquist: efficient sampling of sparse bandlimited signals. IEEE Trans. on Information Theory, 2010, 56(1): 520 – 544.
[5] MISHALI M, ELDAR Y C. Blind multiband signal reconstruction: compressed sensing for analog signals. IEEE Trans. on Signal Processing, 2009, 57(3): 993 – 1009.
[6] QIN Z, WANG J, CHEN J, et al. Adaptive compressed spectrum sensing based on cross validation in wideband cognitive radio system. IEEE Systems Journal, 2017, 11(4): 2422 – 2431.
[7] LIU S, LYU N, WANG H. The implementation of the improved OMP for AIC reconstruction based on parallel index selection. IEEE Trans. on Very Large Scale Integration Systems, 2018, 26(2): 319 – 328.
[8] LASKA J, KIROLOS S, MASSOUD Y, et al. Random sampling for analog-to-information conversion of wideband signals. Proc. of the IEEE Dallas/CAS Workshop on Design, Applications, Integration and Software, 2006: 119 – 122.
[9] KIROLOS S, RAGHEB T, LASKA J, et al. Practical issues in implementing analog-to-information converters. Proc. of the 6th International Workshop on System on Chip for Real Time Applications, 2006: 141 – 146.
[10] VERHELST M, BAHAI A. Where analog meets digital: analog-to information conversion and beyond. IEEE Solid-State Circuits Magazine, 2015, 7(3): 67 – 80.
[11] RAGHEB T, KIROLOS S, LASKA J, et al. Implementation models for analog-to-information conversion via random sampling. Proc. of the 50th Midwest Symposium on Circuits and Systems, 2007: 1 – 4.
[12] TREICHLER J R, DAVENPORT M A, LASKA J N, et al.

Dynamic range and compressive sensing acquisition receivers. Proc. of Defense Applications of Signal Processing, 2011: 1 – 7.
[13] MISHALI M, ELRON A, ELDAR Y C. Sub-Nyquist processing with the modulated wideband converter. Proc. of the IEEE International Conference on Acoustics, Speech and Signal Processing, 2010: 3626 – 3629.
[14] HAQUE T, YAZICIGIL R T, PAN K J L, et al. Theory and design of a quadrature analog-to-information converter for energy-efficient wideband spectrum sensing. IEEE Trans. on Circuits and Systems I: Regular Papers, 2015, 62(2): 527 – 535.
[15] DONOHO D L. For most large underdetermined systems of linear equations the minimal L1-norm solution is also the sparsest solution. Communications on Pure and Applied Mathematics, 2006, 59(6): 797 – 829.
[16] TROPP J A. Algorithms for simultaneous sparse approximation. Part II: convex relaxation. Signal Processing, 2006, 86(3): 589 – 602.
[17] TROPP J A, GILBERT A C, STRAUSS M J. Algorithms for simultaneous sparse approximation. Part I: greedy pursuit. Signal Processing, 2006, 86(3): 572 – 588.
[18] TROPP J A, GILBERT A C. Signal recovery from random measurements via orthogonal matching pursuit. IEEE Trans. on Information Theory, 2007, 53(12): 4655 – 4666.
[19] DO T T, GAN L, NGUYEN N, et al. Sparsity adaptive matching pursuit algorithm for practical compressed sensing. Proc. of the 42nd Asilomar Conference on Signals, Systems and Computers, 2008: 581 – 587.
[20] MALLOY M L, NOWAK R D. Near-optimal adaptive compressed sensing. IEEE Trans. on Information Theory, 2013, 60(7): 4001 – 4012.
[21] SAHOO S K, MAKUR A. Signal recovery from random measurements via extended orthogonal matching pursuit. IEEE Trans. on Signal Processing, 2015, 63(10): 2572 – 2581.
[22] ELDAR Y C, BOLCSKEI H. Block-sparsity: coherence and efficient recovery. Proc. of the IEEE International Conference on Acoustics, Speech and Signal Processing, 2009: 2885 – 2888.
[23] ELDAR Y C, KUPPINGER P, BLCSKEI H. Compressed sensing of block-sparse signals: uncertainty relations and efficient recovery. Mathematics, 2009, 58(6): 3042 – 3054.
[24] FU N, QIAO L Y, CAO L R. Block sparsity adaptive iteration algorithm for compressed sensing. Acta Electronica Sinica, 2011, 39(3A): 75 – 79. (in Chinese)
[25] HEGDE C, BARANIUK R G. Sampling and recovery of pulse streams. IEEE Trans. on Signal Processing, 2010, 59(4): 1505 – 1517.
[26] LI G, ZHU Z, YANG D, et al. On projection matrix optimization for compressive sensing systems. IEEE Trans. on Signal Processing, 2013, 61(11): 2887 – 2898.
[27] DAVENPORT M A, WAKIN M B. Analysis of orthogonal matching pursuit using the restricted isometry propert. IEEE Trans. on Information Theory, 2010, 56(9): 4395 – 4401.
[28] ELDAR Y C, MISHALI M. Block sparsity and sampling over a union of subspaces. Proc. of the 16th International Conference on Digital Signal Processing, 2009: 1 – 8.
[29] XU H, JIANG H, ZHANG C. Multi-narrowband signals receiving method based on analog-to-information convertor and block sparsity. Journal of Systems Engineering and Electronics, 2017, 28(4): 643 – 653.
[30] DAI W, MILENKOVIC O. Subspace pursuit for compressive sensing signal reconstruction. IEEE Trans. on Information Theory, 2009, 55(5): 2230 – 2249.
[31] BJÖRK A. Numerical methods for least squares problems. Pennsylvania: SIAM, 1996.
[32] CANDES E J, TAO T. Near-optimal signal recovery from random projections: universal encoding strategies? IEEE Trans. on Information Theory, 2006, 52(12): 5406 – 5425.

Biographies

ZHANG Chaozhu was born in 1970. He received his B.S. degree in electronics and information engineering from Harbin Institute of Technology in 1993, M.S. degree in communications and information systems and Ph.D. degree in signal and information processing from Harbin Engineering University in 2002 and 2006 respectively. He is a professor with Harbin Engineering University, China. He is a member of IEEE, academician of Chinese Aerospace Society and Heilongjiang Biomedical Engineering Society. His researches include signal processing applications in radar and communications and image processing.
E-mail: zhangchaozhu@hrbeu.edu.cn

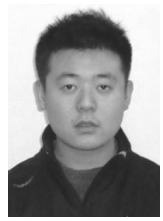

XU Hongyi was born in 1992. He received his B.Eng. degree in electronic and information engineering, from Harbin Engineering University, Harbin, China, in 2014. He is currently working towards his M.Eng. and Ph.D. degrees in information and communication engineering at Harbin Engineering University, Harbin, China. His research interests include radar signal processing and compressive sensing. He is currently participating academic exchange in Beijing Institute of Technology.
E-mail: xhyxwxag@126.com

JIANG Haiqing was born in 1981. He received his B.Eng. and Ph.D. degrees, both in signal and information processing, from the Beijing Institute of Technology, Beijing, China, in 2003 and 2008, respectively. He is currently working as a lecturer in School of Information and Electronics at Beijing Institute of Technology. His research interests include radar signal processing and digital receiver technology.
E-mail: haiqingd99@bit.edu.cn